

# Non-Fourier Heat Conduction in Carbon Nanotubes

Hai-Dong Wang

Bing-Yang Cao

Zeng-Yuan Guo<sup>1</sup>

e-mail: demgzy@tsinghua.edu.cn

Key Laboratory for Thermal Science and Power  
Engineering of Ministry of Education,  
Department of Engineering Mechanics,  
Tsinghua University,  
Beijing 100084, China

*Fourier's law is a phenomenological law to describe the heat transfer process. Although it has been widely used in a variety of engineering application areas, it is still questionable to reveal the physical essence of heat transfer. In order to describe the heat transfer phenomena universally, Guo has developed a general heat conduction law based on the concept of thermomass, which is defined as the equivalent mass of phonon gas in dielectrics according to Einstein's mass-energy relation. The general law degenerates into Fourier's law when the thermal inertia is neglected as the heat flux is not very high. The heat flux in carbon nanotubes (CNTs) may be as high as  $10^{12}$  W/m<sup>2</sup>. In this case, Fourier's law no longer holds. However, what is estimated through the ratio of the heat flux to the temperature gradient by molecular dynamics (MD) simulations or experiments is only the apparent thermal conductivity (ATC); which is smaller than the intrinsic thermal conductivity (ITC). The existing experimental data of single-walled CNTs under the high-bias current flows are applied to study the non-Fourier heat conduction under the ultrahigh heat flux conditions. The results show that ITC and ATC are almost equal under the low heat flux conditions when the thermal inertia is negligible, while the difference between ITC and ATC becomes more notable as the heat flux increases or the temperature drops. [DOI: 10.1115/1.4005634]*

*Keywords: non-Fourier heat conduction, thermomass, carbon nanotubes, thermal conductivity*

## 1 Introduction

Fourier's law of heat conduction has been proved valid by numerous experiments and widely used in a variety of engineering areas, although it is only a phenomenological law which describes the essence of heat diffusion. Onsager once pointed out that [1] "We recognize that Fourier's law is only an approximate description of the process of conduction, neglecting the time needed for acceleration of the heat flow." It is seen that Fourier's law contradicts the principle of the microscopic reversibility in thermodynamics. Furthermore, the time needed for acceleration of the heat flow can be understood as the thermal "inertia," i.e., the lag effect of the gradually increased heat flux after the establishment of the temperature gradient. The thermal inertia is much like the other forms of inertia existed between ubiquitous generalized fluxes and forces [2]. The thermal wave induced by the temporal thermal inertia has been studied in detail by many researchers [3,4]. Later the hyperbolic heat conduction–radiation problem has been studied using lattice Boltzmann method [5]. But it is only the appearance of thermal inertia in the unsteady state, the thermal inertia is not fully described. There has been no universal quantitative analysis of the thermal inertia until the development of the concept of "thermomass" by Cao and Guo [6]. Based on the thermomass model, a general heat conduction law has been created. The thermal wave phenomena can be well described in the thermomass model [7]. Fourier's law is only the special case of the general heat conduction law when the thermal inertia is negligible.

According to Einstein's mass–energy relation, the equivalent mass of phonon gas in dielectrics is referred to as the thermomass. Because the drift velocity of phonon gas is quite small compared to the speed of light, the Newtonian mechanics is applicable to the thermomass. The momentum conservation equation for the motion of the phonon gas/thermomass is actually referred to as the general heat conduction law. In most cases, the thermal inertia

could be ignored when the heat pulse duration is not extremely short or the heat flux is not extremely high. But in CNTs under extreme conditions, some non-Fourier heat conduction behaviors will be revealed due to the effect of thermal inertia. In unsteady state, Shiomi and Maruyama [8] studied the wavelike non-Fourier heat conduction in CNTs heated by subpicosecond pulsed lasers using molecular dynamics simulations. In steady state, Pop et al. [9] measured the thermal conductivity of a single-walled carbon nanotube using an electrical self-heating method under high-bias current flows. The heat flux could be as high as  $10^{12}$  W/m<sup>2</sup>. The results showed that the average temperature over the nanotube deviated from that predicted by Fourier's law with a constant thermal conductivity. Vikram et al. [10] measured the temperature profiles along an electrically heated individual suspended CNT using a spatially resolved Raman spectra method. The significant temperature jumps at the ends of the nanotube were observed, which was only explained with the contact thermal resistance. Based on the thermomass theory, these experimental results provide us some evidences for the existence of the thermal inertia in the steady heat conduction. This article intends to reveal these non-Fourier phenomena in CNTs under the ultrahigh heat flux conditions based on the general heat conduction law.

## 2 Equation of Motion for Phonon Gas

Phonon is the energy quantum of the quantized lattice vibration energy, and the state of the thermal vibration energy of lattice can be characterized as a phonon gas consisting of a large number of randomly moving phonons [11]. Hence, as the smallest transfer unit of the lattice thermal energy, the phonon is the main energy carrier of the heat conduction in the dielectrics. The equivalent mass of phonon gas, referred to as the thermomass, was derived from Einstein's mass–energy relation by Guo et al. [12] as

$$M_h = \frac{E_{D0}}{c^2} \quad (1)$$

where  $M_h$  is the equivalent mass of phonon gas,  $c = 3.0 \times 10^8$  m/s is the speed of light in vacuum, and  $E_{D0}$  is the thermal vibration energy.

<sup>1</sup>Corresponding author.

Contributed by the Heat Transfer Division of ASME for publication in the JOURNAL OF HEAT TRANSFER. Manuscript received April 12, 2010; final manuscript received November 4, 2010; published online April 11, 2012. Assoc. Editor: Ping Cheng.

In addition, Cao [6] established a state equation of the phonon gas in the dielectrics as

$$P_h = \gamma \rho_h C T = \frac{\gamma \rho}{c^2} (C T)^2 \quad (2)$$

where  $\gamma$ ,  $C$ ,  $T$ ,  $\rho$ ,  $P_h$ , and  $\rho_h$  represent the Grüneisen coefficient, specific heat, temperature, density of the dielectrics, pressure, and density of the phonon gas, respectively. Here, the density of the phonon gas is  $\rho_h = \frac{\rho C T}{c^2}$ . It is noted that Eq. (2) is very similar to the state equation of an ideal gas.

The Grüneisen coefficient of phonon gas is the isometric proportion factor of the phonon gas pressure to the thermal energy. Just like the Grüneisen coefficient of dielectrics,  $\gamma$  will decrease as the degree of compression of phonon gas increases. The Grüneisen coefficients in Fig. 1 are calculated by the experimental results from Ref. [9]. Here, the degree of compression is defined as  $\delta = \rho_h / \rho_{h0} = T / T_0$  ( $T_0$  is the ambient temperature).

In Newtonian mechanics, one can obtain the mass and momentum conservation equations of the phonon gas as

$$\frac{\partial \rho_h}{\partial t} + \rho_h \frac{\partial u_h}{\partial x} + u_h \frac{\partial \rho_h}{\partial x} = \frac{S}{c^2} \quad (3a)$$

$$\rho_h \left( \frac{\partial u_h}{\partial t} + u_h \frac{\partial u_h}{\partial x} \right) + u_h \frac{S}{c^2} + \frac{\partial P_h}{\partial x} + f_h = 0 \quad (3b)$$

where  $S$  is the internal heat source,  $u_h = \frac{q}{\rho C T}$  is the drift velocity of the phonon gas. In one-dimensional steady states without internal heat sources, the momentum conservation equation (3b) can be simplified as [6]

$$\rho_h u_h \frac{du_h}{dx} + \frac{dP_h}{dx} + f_h = 0 \quad (4)$$

The three terms on the left side of Eq. (4) are the inertia force, driving force and resistance of the phonon gas, respectively. When the heat flux is not extremely high and the inertia force term is ignored, Eq. (4) will reduce to Fourier's law (see Eq. (5)). Here, the first-order resistance  $f_h = \beta u_h$  is used, in which  $\beta = \frac{2\gamma \rho^2 C^3 T^2}{K c^2}$

$$\frac{dP_h}{dx} + f_h = 0 \Rightarrow K \frac{dT}{dx} + q = 0 \quad (5)$$

where  $K$  is the ATC. It is seen that Fourier's law is the equivalent relationship between the driven force and resistance of the thermomass.

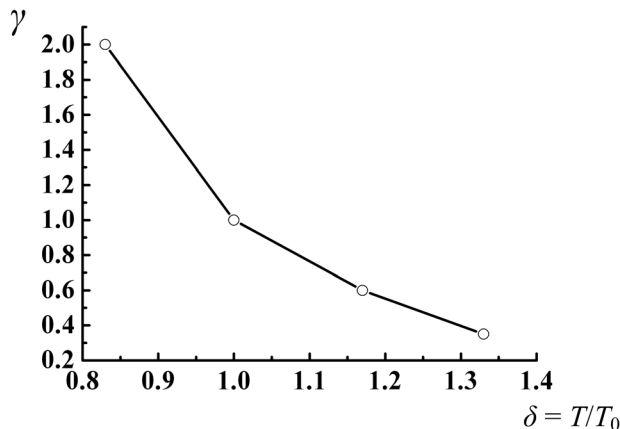


Fig. 1 Variation of Grüneisen coefficient of phonon gas versus the degree of compression

In one-dimensional steady states with constant internal heat sources, the general heat conduction law could be obtained from the mass and momentum conservation Eqs. (3a) and (3b) as

$$\begin{aligned} & \left( \frac{-K_I q S}{\gamma \rho^2 C^3 T^3} \frac{\partial T}{\partial x} + \frac{K_I q^2}{2\gamma \rho^2 C^3 T^4} \left( \frac{\partial T}{\partial x} \right)^2 \right) \\ & + \frac{K_I}{\gamma \rho C^2 T} \left( \frac{S}{\rho C T} - \frac{q}{\rho C T^2} \frac{\partial T}{\partial x} \right) \left( S - \frac{q}{T} \frac{\partial T}{\partial x} \right) \\ & + K_I \left( 1 - \frac{q^2}{2\gamma \rho^2 C^3 T^3} \right) \frac{\partial^2 T}{\partial x^2} + S = 0 \end{aligned} \quad (6)$$

where  $K_I$  is the ITC. To simplify the Eq. (6), we assume  $q \approx -K_I \frac{\partial T}{\partial x} \approx \frac{1}{2} S L$  and then get the simplified form as

$$K_I \left( 1 - \frac{q^2}{2\gamma \rho^2 C^3 T^3} \right) \frac{d^2 T}{dx^2} + \left( 1 + \frac{\varepsilon K_I S}{\gamma \rho^2 C^3 T^2} \right) S \approx 0 \quad (7)$$

The parameter  $\varepsilon = \frac{\beta_s^*}{4} + \frac{\beta_s^{*2}}{32} + \left( 1 + \frac{\beta_s^*}{4} \right)^2$  and the dimensionless number  $\beta_s^* = \frac{S L^2}{T K_I}$ , where  $L$  is the characteristic length. It is seen that Fourier's law is an approximation to the general heat conduction law when the thermal inertia is ignored. The thermomass theory reveals the mass nature of heat and connects the heat conduction to the other mass transport phenomena.

### 3 Second-Order Resistance of Thermomass

The phonon gas flow in dielectrics is much like the gas flow in porous media, and they have the similar governing equations (see Eqs. (3a) and (3b)). The drift velocity of the phonon gas is usually quite small. For instance, the drift velocity in carbon is about  $10^{-4}$  m/s when the heat flux is  $10^5$  W/m<sup>2</sup>. In this case, the first-order resistance  $f_h = \beta u_h$  is appropriate, where  $\beta$  is the proportional coefficient. But the drift velocity increases with the increasing heat flux, the resistance formula may deviate from the first-order relation when the drift velocity is quite high. Here, we apply the second-order modification to the resistance of thermomass.

The dimensionless resistance could be defined as  $F_h = \beta_1^* U_h + \frac{1}{2} \beta_2^* U_h^2 + \frac{1}{6} \beta_3^* U_h^3 + \dots$ , where  $F_h = \frac{L}{P_{h0}} f_h$ ,  $P_{h0} = \frac{\gamma \rho C^2 T_0^2}{c^2}$ . The second-order resistance is written as

$$f_h \approx \frac{P_{h0}}{L} \left( \beta_1^* U_h + \frac{1}{2} \beta_2^* U_h^2 \right) = \beta_1 u_h + \beta_2 u_h^2 \quad (8)$$

The first-order resistance coefficient is  $\beta_1 = \frac{2\gamma \rho^2 C^3 T^2}{K_I c^2}$ ,  $\beta_1^* = \frac{T^2}{T_0^2}$ . Similarly, the second-order resistance coefficient is  $\beta_2 = \beta_2^* \frac{2\gamma \rho^3 C^4 T_0^2 L}{K_I^2 c^2}$ ,  $\beta_2^* = -\beta_{h2}^* \frac{T^2}{T_0^2}$ . Then, the governing equation of thermomass with second-order resistance could be obtained as

$$K_I \left( 1 - \frac{q^2}{2\gamma \rho^2 C^3 T^3} \right) \frac{d^2 T}{dx^2} + \left( 1 + \frac{\varepsilon K_I S}{\gamma \rho^2 C^3 T^2} - \beta_{h2}^* \frac{L^2 S}{T K_I} \right) S \approx 0 \quad (9)$$

If we set  $\beta_h^{**} = -\frac{8\varepsilon(1-\eta)}{\beta_s^{*2}} + \beta_{h2}^*$ , where the coefficient  $\eta = \frac{K}{K_I} = 1 - \frac{q^2}{2\gamma \rho^2 C^3 T^3}$ , ( $0 \leq \eta \leq 1$ ) is the ratio of the ATC to the ITC. Then, the general heat conduction law with second-order resistance of thermomass in steady states could be written as

$$K_I \left( 1 - \frac{q^2}{2\gamma \rho^2 C^3 T^3} \right) \frac{d^2 T}{dx^2} + (1 - \beta_h^{**} \beta_s^*) S \approx 0 \quad (10)$$

It is clear that if we set  $\eta = 1$  and  $\beta_{h2}^* = 0$ , Eq. (10) will reduce to Fourier's law.

#### 4 Heat Flow Choking Under Ultrahigh Heat Flux

The unsteady motion equation without internal heat source could be written as

$$\rho\tau C \frac{\partial^2 T}{\partial t^2} + \rho C \frac{\partial T}{\partial t} = K_I \left( 1 - \frac{\rho C \tau u_h^2}{K_I} \right) \frac{\partial^2 T}{\partial x^2} - \frac{K_I u_h}{\gamma C T} \frac{\partial^2 T}{\partial t \partial x} \quad (11)$$

where  $\tau = \frac{K_I}{2\gamma\rho C^2 T}$  has a unit of time, corresponding to the relaxation time in Cattaneo-Vernotte (C-V) model, and is usually in order of magnitude of  $10^{-10}$  s. Here, we assume that the time scale is much larger than the relaxation time and the thermal equilibrium state can be reached. This assumption is valid in most cases. Usually  $\frac{\rho C \tau u_h^2}{K_I} \ll 1$ , the thermal sound speed (propagation speed of the thermal disturbance) in the phonon gas can be expressed as

$$C_h = \sqrt{\frac{K_I}{\rho C \tau}} = \sqrt{2\gamma C T} \quad (12)$$

Tzou [13] investigated the thermal shock phenomena caused by an ultrafast moving heat source in a solid as the speed of the heat source exceeds the thermal sound speed. Experimental evidence has been found by studying the temperature distribution around a rapidly propagating crack tip [14]. Based on the thermal wave theory, a thermal Mach number has been brought forward

$$\text{Ma} = \frac{u_s}{C_h} \quad (13)$$

where  $u_s$  is the speed of the internal heat source and  $C_h$  is the thermal sound speed.

Likewise, we defined the ratio of the drift velocity of the phonon gas to the thermal sound speed as the thermal Mach number as

$$\text{Ma}_h = \frac{u_h}{C_h} \quad (14)$$

Then, Eq. (10) can be rewritten as

$$K_I (1 - \text{Ma}_h^2) \frac{d^2 T}{dx^2} + (1 - \beta_h^{**} \beta_s^{**}) S = 0 \quad (15)$$

Based on the general heat conduction law, the non-Fourier behaviors in CNTs under ultrahigh heat flux conditions can be studied. For a CNT electrically heated by high-bias current flows (see Fig. 2), the drift velocity of the phonon gas increases in the nanotube as the phonon gas density  $\rho_h$  decreases along the heat flow direction, just like the gas flow in a converging nozzle.

According to the knowledge of aerodynamics, the flow status of the converging nozzle is controlled by the Mach number at the outlet. The flow choking will happen when the Mach number reaches unity. In the case of phonon gas, the drift velocity increases with the increasing heat flux/internal heat source. After the thermal Mach number reached unity, increasing heat flux/in-

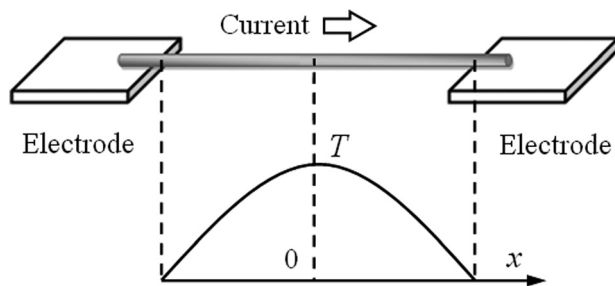


Fig. 2 An electrically heated CNT suspended between two electrodes with a typical parabolic temperature profile

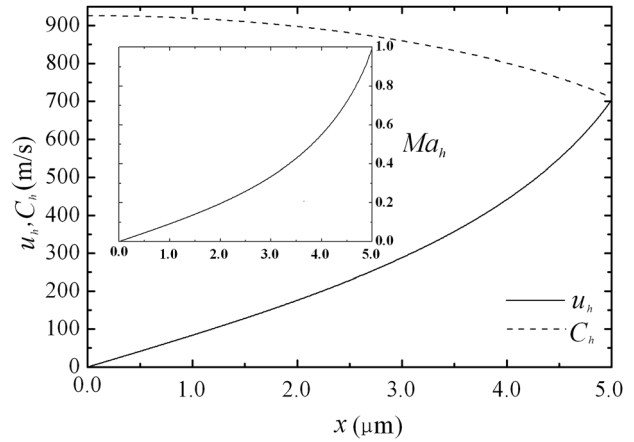


Fig. 3 The drift velocity and thermal sound speed in the CNT

ternal heat source will lead to the heat flow choking in CNTs. Thus, a temperature jump  $\Delta T = \sqrt[3]{q^2 / (2\gamma\rho^2 C^3)} - T_0$  will occur at the nanotube end, and the heat flux in this case is referred to as the critical heat flux  $q_c = \sqrt{2\gamma\rho^2 C^3 T_0^3}$ .

The following parameters of the single-walled CNTs are used in the calculations: the density  $\rho = 2200$  kg/m<sup>3</sup>, the specific heat  $C = 500$  J/kg K, the thermal conductivity  $K_I = 3000$  W/mK, the diameter  $D = 1.8$  nm, the length  $L = 10$  μm, the electrode temperature  $T_0 = 300$  K, and the heating power  $S = 1.5$  μW (the critical heat flux is  $1.8 \times 10^{11}$  W/m<sup>2</sup>, which corresponds to the heating power of  $S = 0.7$  μW). The cross-sectional area is calculated as  $A = \pi D d$ , in which the nanotube wall thickness  $d = 0.34$  nm.

The inset in Fig. 3 shows the increasing thermal Mach number along the nanotube length.

Since the heat flux of  $3.9 \times 10^{11}$  W/m<sup>2</sup> in the present calculation is much higher than the critical heat flux of  $1.8 \times 10^{11}$  W/m<sup>2</sup>, the drift velocity is as high as 700 m/s at the nanotube end (see Fig. 3). Also, a significant temperature jump about 200 K occurs at the nanotube end shown in Fig. 4. The temperature profile based on Fourier's law is much lower than that based on the general heat conduction law.

The average temperatures over the nanotube are calculated with a constant thermal conductivity as shown in Figs. 5 and 6 based on the general heat conduction law and Fourier's law.

A "turning point" is shown in the temperature curve of general heat conduction law, which is due to the heat flow choking. Before the heat flow choking, the average temperature curves based on Fourier's law and general heat conduction law are

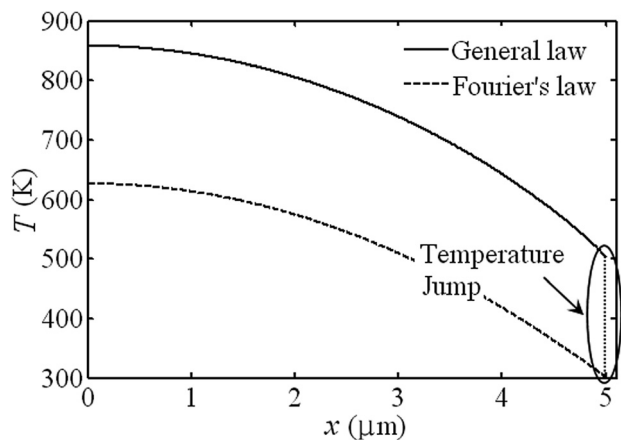


Fig. 4 Temperature profiles calculated based on the general law and Fourier's law

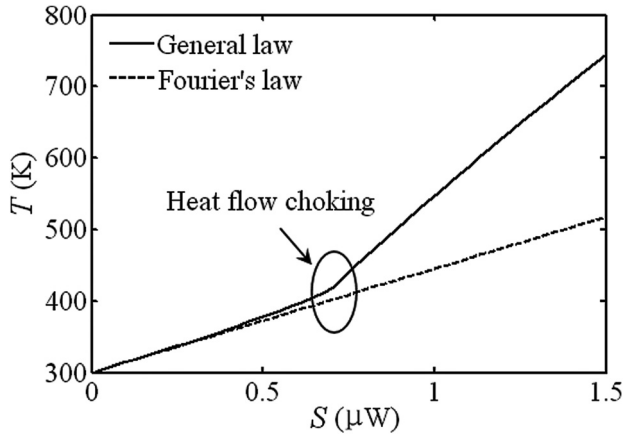


Fig. 5 Variation of the average temperature of the nanotube versus the heating power

almost the same. Nevertheless, after the turning point, the average temperature from general heat conduction law is higher than that from Fourier's law because of the temperature jump at the nanotube end. This difference increases with the increasing heating power.

The experimental data from Ref. [9] are used to compare with the results from Fourier's law and general heat conduction law. The experimental average temperatures are calculated by the Landauer-Büttiker approach [15,16]

$$R(V, T) = R_c + \frac{h}{4q_e^2} \frac{L + \lambda_{\text{eff}}(V, T)}{\lambda_{\text{eff}}(V, T)} \quad (16a)$$

$$\lambda_{\text{eff}} = \left( \lambda_{AC}^{-1} + \lambda_{OP,ems}^{-1} + \lambda_{OP,abs}^{-1} \right)^{-1} \quad (16b)$$

where  $h$ ,  $q_e$ ,  $\lambda_{\text{eff}}$  are the Planck constant, elementary charge, and effective electron mean free path.  $h/(4q_e^2) \approx 6.5\text{K}\Omega$  is the quantum contact resistance.

It is seen that temperature curves predicted by the general heat conduction law (solid line in Fig. 6) agree well with the experimental results. Of course, there are still some differences between the predicted temperatures by the general heat conduction law and the experimental data, which may come from the temperature dependence of the ITC of the CNTs.

## 5 Apparent and Intrinsic Thermal Conductivities

As mentioned above, the thermal conductivity gained from MD simulations or experimental results is normally based on Fourier's

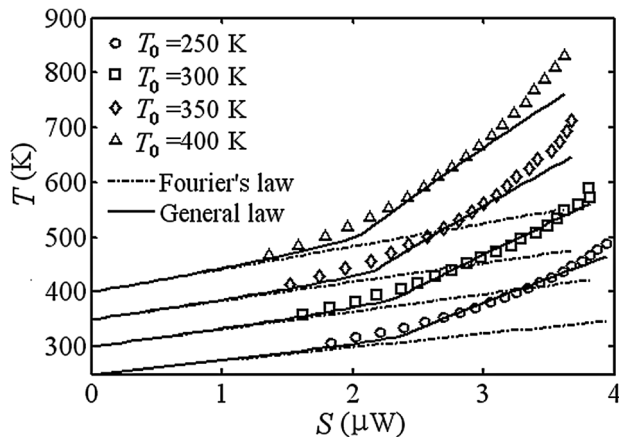


Fig. 6 Average temperatures based on the general law and Fourier's law using the existing experimental data from Ref. [9]

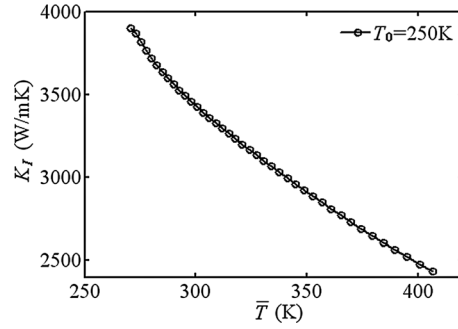


Fig. 7 ITC calculated from Ref. [9] under  $T_0 = 250\text{ K}$

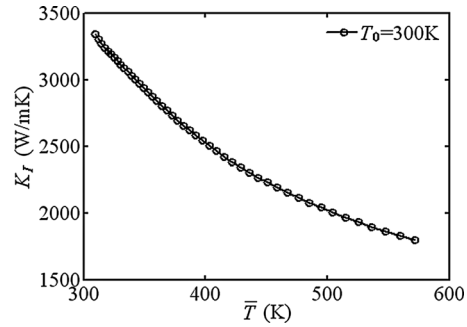


Fig. 8 ITC calculated from Ref. [9] under  $T_0 = 300\text{ K}$

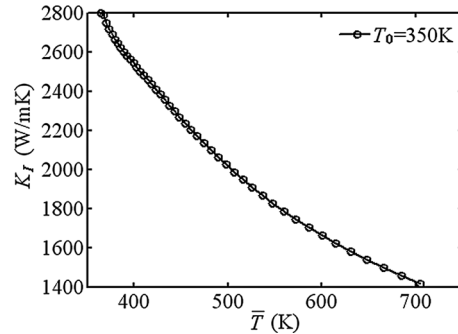


Fig. 9 ITC calculated from Ref. [9] under  $T_0 = 350\text{ K}$

law, which is in fact the ATC. The ITC can only be gained by the general heat conduction law (see Eq. (10)). The relation between ATC and ITC is shown as

$$K = K_I \left( 1 - \frac{q^2}{2\gamma\rho^2 C^3 T^3} \right) \quad (17)$$

The ITC is the thermal conductivity when the thermal inertia is negligible. ATC is equal to ITC when the heat flux is not very high, but the difference will be notable in CNTs under the ultrahigh heat flux conditions, especially after the heat flow choking.

The ITCs shown in Figs. 7–10 are numerically determined by the thermomass motion equation (10) with second-order resistance. The abscissa  $\bar{T}$  is the average temperature over the nanotube. It is seen that ITCs under different ambient temperatures follow the same varying tendency in 250 K~800 K. Furthermore, the comparison between ATC and ITC is shown in Figs. 11 and 12, where ATCs are numerically determined by Fourier's law.

It is clear that ATC and ITC are equal when the heating power is less than  $2\ \mu\text{W}$  in this case. After the heat flow choking, the difference will increase with the increasing heating power. That also means the thermal inertia could not be ignored in CNTs under the ultrahigh heat flux conditions.

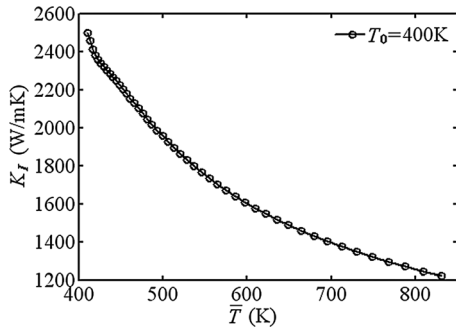


Fig. 10 ITC calculated from Ref. [9] under  $T_0 = 400$  K

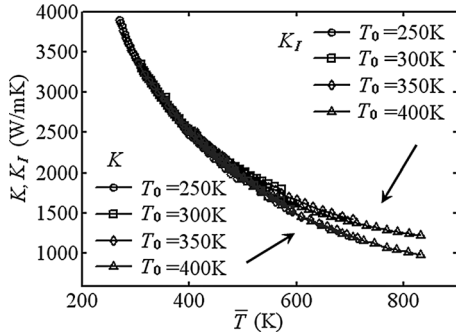


Fig. 11 ATC with varied temperature and heating power

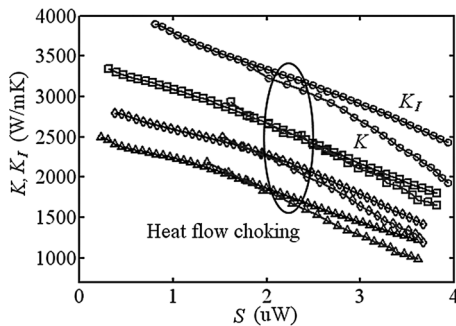


Fig. 12 ITC with varied temperature and heating power

## 6 Concluding Remarks

- (1) According to Einstein's mass-energy relation, the equivalent mass of the thermal energy of phonon gas is defined as thermomass. We obtain the momentum conservation equation of thermomass based on Newtonian mechanics, which can be regarded as the general heat conduction law.
- (2) Under normal conditions, the general heat conduction law will reduce to Fourier's law, since the thermal inertia is negligible. But the heat flux could be ultrahigh in CNTs, the effect of thermal inertia will lead to the non-Fourier behaviors in CNTs.
- (3) The phonon gas flow in a CNT is like the gas flow in a converging nozzle. The heat flux is choked as the temperature and the heat flux at the nanotube end exceed the critical values, since the thermal Mach number at the nanotube end cannot be greater than unity. Meanwhile, temperature jumps occur at the nanotube ends in this case.
- (4) The thermal conductivity calculated by Fourier's law is only the ATC, which is smaller than the ITC based on the general heat conduction law. ATC and ITC are almost equal when

the thermal inertia is negligible. But as the heating power increases, the difference between ATC and ITC will be more notable especially when the heat flow choking occurs.

## Acknowledgment

The work described in this paper was supported by the National Natural Science Foundation of China (Grant Nos. 51076080 and 51136001).

## Nomenclature

$A$  = cross-sectional area  
 $c$  = light speed  
 $C$  = specific heat  
 $C_h$  = thermal sound speed  
 $d$  = nanotube wall thickness  
 $D$  = nanotube diameter  
 $E_{D0}$  = thermal vibration energy  
 $f_h$  = resistant force of phonon gas  
 $F_h$  = dimensionless resistant force of phonon gas  
 $h$  = Planck constant  
 $K$  = apparent thermal conductivity  
 $K_I$  = intrinsic thermal conductivity  
 $L$  = nanotube length  
 $Ma$  = Mach number  
 $Ma_h$  = thermal Mach number  
 $M_h$  = thermomass  
 $P$  = pressure  
 $P_h$  = phonon gas pressure  
 $P_{h0}$  = characteristic phonon gas pressure  
 $q$  = heat flux  
 $q_c$  = critical heat flux  
 $q_e$  = elementary charge  
 $R$  = electric resistance  
 $R_c$  = quantum contact resistance  
 $S$  = internal heat source  
 $t$  = time variable  
 $T$  = temperature  
 $T_0$  = ambient temperature  
 $u_h$  = drift velocity of phonon gas  
 $U_h$  = dimensionless drift velocity of phonon gas  
 $V$  = voltage  
 $x$  =  $x$  space variable

## Greek Symbols

$\beta$  = coefficient of phonon gas resistant force  
 $\beta_1$  = first-order coefficient  
 $\beta_2$  = second-order coefficient  
 $\beta_1^*$  = dimensionless first-order coefficient  
 $\beta_2^*$  = dimensionless second-order coefficient  
 $\beta_s^*$  = dimensionless internal heat source number  
 $\beta_h^{**}$  = total dimensionless coefficient of phonon gas resistant force  
 $\gamma$  = Grüneisen coefficient  
 $\delta$  = degree of compression  
 $\varepsilon$  = integral parameter  
 $\eta$  = ratio of the apparent thermal conductivity to the intrinsic thermal conductivity  
 $\lambda_{\text{eff}}$  = effective electron mean free path  
 $\rho$  = density  
 $\rho_h$  = density of phonon gas  
 $\rho_{h0}$  = characteristic density of phonon gas  
 $\tau$  = characteristic time

## Superscript

\* = dimensionless parameter

## Subscript

$h$  = thermomass

## References

- [1] Onsager, L., 1931, "Reciprocal Relations in Irreversible Processes," *Phys. Rev.*, **37**, pp. 405–426.
- [2] Sieniutycz, S., 2002, "Relativistic Thermo-Hydrodynamics and Conservation Laws in Continua With Thermal Inertia," *Rep. Math. Phys.*, **49**, pp. 361–370.
- [3] Joseph, D. D., and Preziosi, L., 1989, "Heat Waves," *Rev. Mod. Phys.*, **61**, pp. 41–73.
- [4] Joseph, D. D., and Preziosi, L., 1990, "Addendum to the Paper 'Heat Waves,'" *Rev. Mod. Phys.*, **62**, pp. 375–391.
- [5] Mishra, S. C., and Kumar, T. B. P., 2009, "Analysis of a Hyperbolic Heat Conduction-Radiation Problem With Temperature Dependent Thermal Conductivity," *ASME J. Heat Transfer*, **131**, p. 111302.
- [6] Cao, B. Y., and Guo, Z. Y., 2007, "Equation of Motion of a Phonon Gas and Non-Fourier Heat Conduction," *J. Appl. Phys.*, **102**, p. 053503.
- [7] Guo, Z. Y., and Hou, Q. W., 2010, "Thermal Wave Based on the Thermomass Model," *ASME J. Heat Transfer*, **132**, p. 072403.
- [8] Shiomi, J., and Maruyama, S., 2006, "Non-Fourier Heat Conduction in a Single-Walled Carbon Nanotube: Classical Molecular Dynamics Simulations," *Phys. Rev. B*, **73**, p. 205420.
- [9] Pop, E., Mann, D., Wang, Q., Goodson, K., and Dai, H., 2006, "Thermal Conductance of a Single-Walled Carbon Nanotube Above Room Temperature," *Nano Lett.*, **6**, pp. 96–100.
- [10] Vikram, V. D., Scott, H., Adam, W. B., Marc, B., and Stephen, B. C., 2009, "Spatially Resolved Temperature Measurements of Electrically Heated Carbon Nanotubes," *Phys. Rev. Lett.*, **102**, p. 105501.
- [11] Kittel, C., Xiang, J. Z., and Wu, X. H., 2005, *Introduction to Solid State Physics*, Chemical Industry Press, Beijing.
- [12] Guo, Z. Y., Cao, B. Y., Zhu, H. Y., and Zhang, Q. G., 2008, "A General Heat Conduction Law Based on the Concept of Motion of Thermal Mass," *Acta Phys. Sin.*, **57**, pp. 4273–4281 (in Chinese).
- [13] Tzou, D. Y., 1989, "Shock Wave Formation Around a Moving Heat Source in a Solid With Finite Speed of Heat Propagation," *Int. J. Heat Mass Transfer*, **32**, pp. 1979–1987.
- [14] Tzou, D. Y., 1992, "The Thermal Shock Phenomena Induced by a Rapidly Propagating Crack Tip: Experimental Evidence," *Int. J. Heat Mass Transfer*, **35**, pp. 2347–2356.
- [15] Pop, E., Mann, D., Reifenberg, J., Goodson, K., and Dai, H., 2005, "Electro-Thermal Transport in Metallic Single-Wall Carbon Nanotubes for Interconnect Applications," International Electron Devices Meeting, Washington, DC.
- [16] Pop, E., Mann, D., Cao, J., Wang, Q., Goodson, K., and Dai, H., 2005, "Negative Differential Conductance and Hot Phonons in Suspended Nanotube Molecular Wires," *Phys. Rev. Lett.*, **95**, p. 155505.